Materials Science and Engineering A 528 (2011) 815–822

Contents lists available at ScienceDirect

Materials Science and Engineering A

journal homepage: www.elsevier.com/locate/msea

Nanoindentation and XRD investigations of single crystalline Ni–Ge brazed nickel-base superalloys PWA 1483 and René N5

S. Neumeier[a,*,1], M. Dinkel[a,2], F. Pyczak[b], M. Göken[a]

[a] Department of Materials Science & Engineering, Institute I, University Erlangen-Nürnberg, 91058 Erlangen, Germany
[b] Institute for Materials Research, GKSS Research Centre Geesthacht, 21502 Geesthacht, Germany

ARTICLE INFO

Article history:
Received 4 April 2010
Received in revised form 27 July 2010
Accepted 22 September 2010

Keywords:
Nanoindentation
X-ray diffraction
Nickel based superalloys
Diffusion brazing

ABSTRACT

Two single crystal nickel-base superalloys of the first and second generation (PWA 1483 and René N5) were diffusion brazed with two different germanium containing brazing materials which were optimised for each alloy. The two-phase microstructure of the single crystalline brazing joint consists of a γ′ precipitate phase embedded in a γ matrix.

The local mechanical properties of the γ- and γ′-phases and the lattice misfit of single crystalline nickel-base superalloy brazing joints were measured over the joint region and the surrounding base material. The results for both systems show strong differences in the properties with respect to local chemical composition, hardness and lattice constants. The γ-phase in the joint center and the base material has almost the same hardness, whereas a large difference was found for the γ′-phases respectively. In both alloys the hardness of the γ′-phase in the base material was about 15% higher than in the joint. The lattice misfit at room temperature was negative in both base materials. In case of the brazing joint of René N5 a positive lattice misfit was measured, while the PWA 1483 joint shows a negative misfit in the former gap center. Accordingly the microstructural evolution of each brazing joint shows significant differences during creep.

1. Introduction

Due to the high cost of single crystalline (SX) nickel-base superalloy components the development of joining techniques for turbine blades and the development of repair processes for fatigue cracks is a worthwhile goal. Research on the applicability of transient liquid phase bonding (TLP) for joining and repair of such materials has shown a high potential of this method for both purposes [1,2]. TLP-bonding is a process where gap closure is achieved by isothermal solidification of the braze. The solidification takes place due to the outward diffusion of the so called melting point depressing element, which lowers the melting point of the braze alloy. By diffusion into the base material the melting point of the liquid braze increases at the solid liquid interface and the material solidifies. By this process the brazing zone can solidify fully from outward to inward when enough time is allowed for the diffusion process to take place. This process allows closure of the gap in a single crystalline manner. Brazing materials available commercially so far for polycrystalline nickel-base superalloys are boron based. While boron is present as a grain boundary strengthener in many polycrystalline superalloys, the use of boron as a melting point depressing element in nickel-base superalloys can result in the formation of borides. This is unwanted due to their detrimental effects on the fatigue life [3].

Germanium, however, is an efficient melting point depressing element in nickel-base alloys and forms a Ni_3Ge $L1_2$-precipitate phase in the Ni–Ge binary system. These Ni_3Ge precipitates are isomorphous with the regular Ni_3Al based γ′-precipitates present in nickel-base superalloys. Recent work has shown the potential of germanium based brazing alloys [4,5]. Single crystalline joints could be produced and the mechanical properties evaluated in terms of nanoindentation of the joint region and hot tensile tests compared favourably with the substrate material. The results demonstrate a strength level of the joints of about 80–90% of the base materials.

To understand the mechanical behaviour and the microstructural evolution in the joint region a more thorough investigation of the local properties within the joint in terms of the mechanical properties of the γ-matrix phase as well as the γ′-precipitate phase is necessary. This can be accomplished by applying nanoindentation in the atomic force microscope (NI-AFM) which already

* Corresponding author at: Department of Materials Science & Metallurgy, University of Cambridge, UTC, Pembroke Street, Cambridge CB2 3QZ, United Kingdom. Tel.: +44 01223 334367; fax: +44 01223 331956.
E-mail address: sn367@cam.ac.uk (S. Neumeier).
[1] Now at Department of Materials Science & Metallurgy, University of Cambridge, Cambridge CB2 3QZ, UK.
[2] Now at Catalycom GmbH, Badstraße 13-15, 90762 Fürth, Germany.

0921-5093/$ – see front matter © 2010 Elsevier B.V. All rights reserved.
doi:10.1016/j.msea.2010.09.065

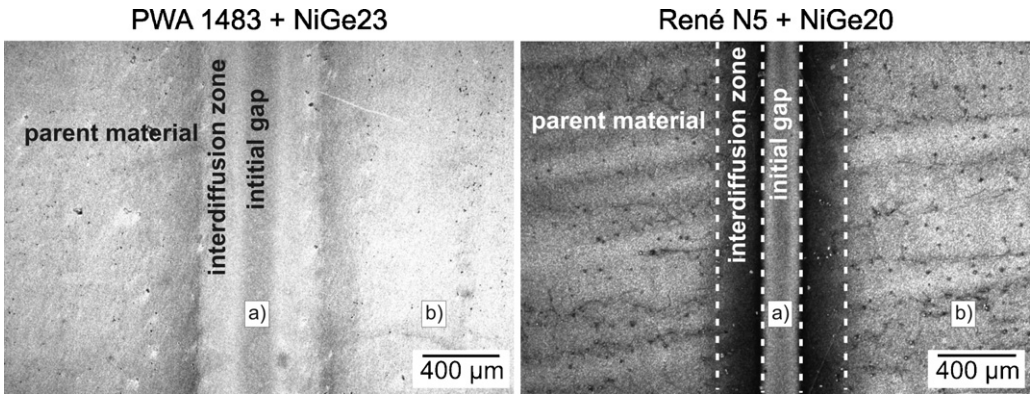

Fig. 1. Light micrograph (dark field images) of the brazing zone of PWA 1483 with NiGe23 and René N5 with NiGe20. The positions where the hardness measurements were performed in the joint area and base material are indicated by letters a and b, respectively.

demonstrated its ability to measure the hardness of the phases γ and γ′ in nickel-base superalloys separately [6–8].

Furthermore the lattice misfit of the joint is measured by X-ray diffraction (XRD). In the two-phase nickel-base superalloys, consisting of the fcc matrix phase (γ) and the coherently embedded $L1_2$ phase (γ′), the lattice misfit δ is defined as

$$\delta = \frac{2(a_{\gamma'} - a_{\gamma})}{a_{\gamma'} + a_{\gamma}} \quad (1)$$

where $a_{\gamma'}$ and a_{γ} denote the lattice parameters of the γ′- and the γ-phases, respectively. The lattice misfit and its magnitude has a profound influence on the microstructural evolution of the γ/γ′-morphology. A negative lattice misfit at high temperatures, which is common for most commercially used nickel-base superalloys, results in the formation of rafts perpendicular to the stress axis under tensile loads and rafts parallel to the stress axis under compressive loads in creep tests [9,10].

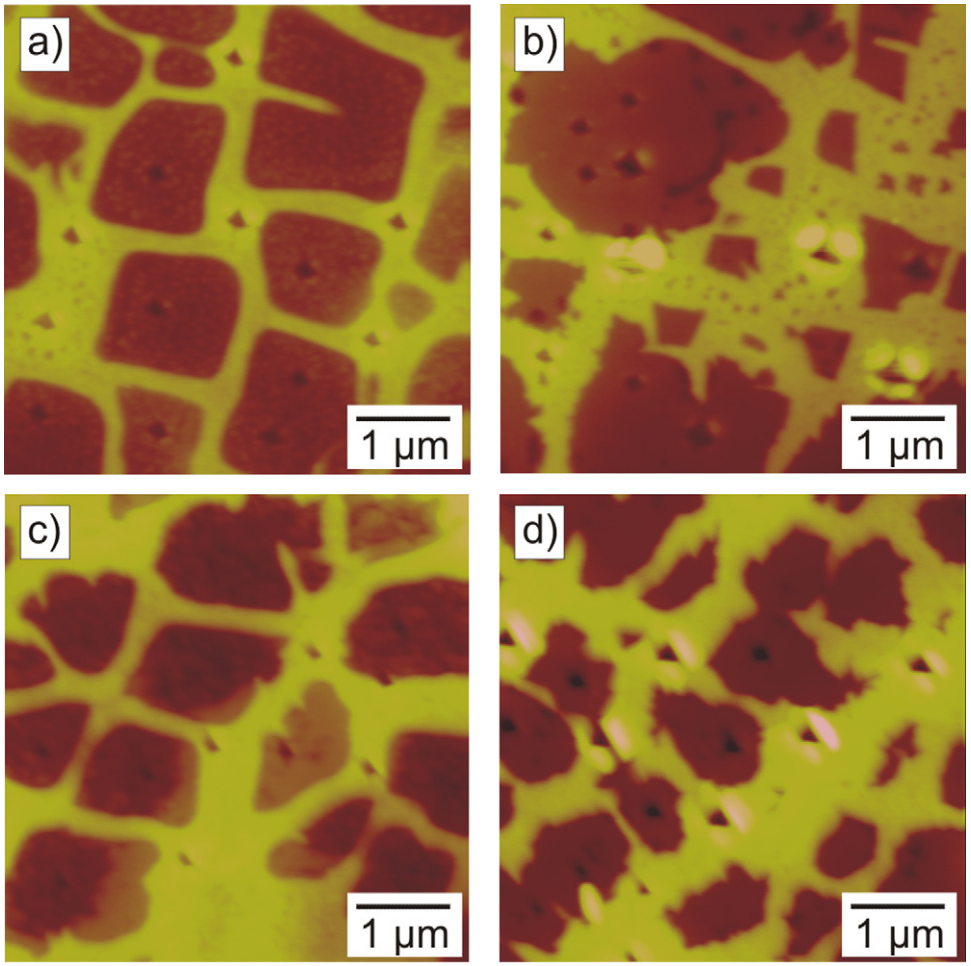

Fig. 2. AFM images of the microstructures after the brazing heat treatment including nanoindents in the γ and γ′ phase: (a) center of the brazing zone of PWA 1483 with NiGe23; (b) base material PWA 1483; (c) center of the brazing zone of René N5 with NiGe20 and (d) base material Rene N5.

Table 1
Chemical compositions of the two parent alloys in wt.%.

Alloys	Ni	Cr	Co	Mo	W	Al	Ti	Ta	Re
PWA 1483	Balance	12.2	9	1.9	3.8	3.6	4.1	5	–
René N5	Balance	7	7.5	1.5	5	6,2	–	6.5	3

2. Experimental

The brazing joints examined in this study were processed at the Institute of Science and Technology of Metals at the University of Erlangen (Prof. R.F. Singer). As base materials the single crystal nickel-base superalloys PWA 1483 and René N5 were used, which are alloys of the first (0 wt.% rhenium) and second generation (3 wt.% rhenium), respectively. Compositions are given in Table 1. Brazing alloys were binary nickel–germanium alloys with 20 wt.% germanium for René N5 and 23 wt.% germanium for PWA 1483, respectively. Subsequently, these combinations are termed PWA 1483 + NiGe23 and René N5 + NiGe20.

The brazing was performed at 1160 °C for 55 h for PWA 1483 + NiGe23 and at 1200 °C for 48 h for Rene N5 + NiGe20. The samples were subsequently furnace cooled to room temperature.

Ideally the initial gap which was brazed is oriented perpendicular to the solidification direction (here [1 0 0]). Details of the process can be found in [5].

The base materials possess a two phase γ/γ′-microstructure. In the pre-brazing condition the γ′-particles are of cuboidal shape with an approximate edge length of about 0.5 μm. The faces of the γ′-cubes are aligned parallel to the ⟨0 0 1⟩ crystallographic directions.

2.1. Nanoindentation

Nanoindentation experiments were performed at room temperature in a Veeco Instruments Multimode atomic force microscope equipped with an add-on Triboscope force transducer from Hysitron. Sample preparation included standard mechanical polishing to 1 μm by using diamond slurry. Final polishing was done with a chemical mechanical polish with 0.125 μm silica slurry. In all indentation experiments a diamond cube corner tip (three sided pyramid) with a tip angle of 90° was used. The benefit of the cube corner indenter is a higher induced plastic strain for a given indentation depth compared with the frequently employed Berkovich indenter. The tip-shape functions, projected area versus indentation depth, were determined with the Oliver/Pharr method [11] by reference indentation in fused silica. The machine compliance was taken into account.

This tip was used for indentation as well as imaging. The indentation of the γ- and γ′-phase in the atomic force microscope has already been shown in various studies [6–8,12]. Due to the small applied loads which lead to indentation depths of just about 50 nm it was possible to measure within the narrow γ-channels of high volume fraction γ′-hardened nickel-base superalloys.

The load and corresponding displacement are recorded continuously during indentation. The hardness H was derived from the nanoindentation experiments by evaluation of the load displacement curve according to the Oliver Pharr method [11]. The hardness H is calculated by

$$H = \frac{P_{\max}}{A_c} \quad (2)$$

where $P_{\max}$ is the maximum force during indentation and A_c the projected contact area. In this case the maximum force was kept constant at 500 μN.

2.2. X-ray diffraction

The XRD measurements were performed with a Philips/Panalytical PW3050/65 X'Pert PRO HR horizontal diffractometer. A Ge (220)-4 bounce primary monochromator was used to monochromatize the X-ray beam using the $K_{\alpha 1}$-radiation for diffraction measurements and eliminate the $K_{\alpha 2}$-radiation. The X-ray beam was narrowed by slits resulting in an irradiated area of about 400 μm in width and a few millimetres in length. The diffracted intensity was recorded with a 3-bounce analyser crystal. The (0 0 2) reflections were detected for each material. They were recorded stepwise from the base material over the joint. Local measurements were done every 50 μm across the joint. Each scan was performed within the 2θ range from 50° to 51.5° with a step size of 0.02°. Although the incident beam size is rather narrow the size of focus area is bigger than the width of the joint. Additionally, the joint is not exactly perpendicular to the solidification direction but deviates by about 7° for PWA 1483 + NiGe23 and 18° in the case of Rene N5 + NiGe20. Accordingly, the irradiated area was not exactly parallel to the joint either, so that data from measurement positions nominally located in the joint area also include some information from the interdiffusion zone.

Nevertheless, it is possible to extract differences in the local lattice parameters of the joint area and the base material.

For the evaluation of the lattice parameters of the two phases γ and γ′ and the calculation of the lattice misfit the XRD-profiles were de-convoluted with two Pseudo-Voigt functions. The ratio of the integrated intensity of the γ- and γ′-subpeaks was chosen 40:60. This corresponds approximately with the γ′-volume fraction in the base material as well as in the joint [4] by assuming that the structure factor of both phases is similar [13].

2.3. EDX-measurements

SEM-EDX measurements were made at a ZEISS Cross Beam 1540 ESB Focused Ion Beam equipped with field emission electron source. The instrument was only used in the scanning electron microscope mode in the present study. EDX measurements were performed with an attached Oxford EDX system. For each data point 25 spots were analysed within the joint region and the base material. For calibration a Co standard was used.

In order to measure the partitioning behaviour of Ge between γ and γ′, TEM-EDX measurements were performed. Due to the complicated preparation efforts necessary to obtain a TEM specimen of the brazing zone this was done exemplarily on a René N5 + NiGe20 sample. The area of interest was prepared as a TEM-lamella using FIB. For the EDX-measurements an Oxford EDX-System was used at a Philips CM200 Transmission Electron Microscope operating at 200 kV acceleration voltage. The nominal spot size was 7 nm and the proprietary Oxford software was used for quantification of the EDX-spectra. The results stem from five measurements in the γ′ phase and five measurements in the γ matrix, respectively.

3. Results

3.1. Microstructure

Light micrographs giving an overview of two brazing zones are shown in Fig. 1. In these micrographs the positions of the nanoindentation experiments are indicated by letters a and b.

Within these micrographs the brazing area can be easily distinguished from the surrounding base material. Additionally besides the indicated former gap, an area with different appearance adja-

cent to the gap can be identified. Due to the diffusion induced changes in chemical composition this area exhibits a modified etching behaviour compared to both the base material and the gap center. No formation of coarse unwanted precipitates of any type can be found within the brazing area.

The microstructures as imaged in the atomic force microscope are shown in Fig. 2 for PWA 1483 and René N5 brazings. The microstructure of the PWA joint, presented in Fig. 2a, shows a relatively homogeneous distribution of the γ′-precipitates within the joint center, whereas the microstructure in the base material exhibits a bimodal particle distribution of coarse as well as fine γ′-particles (Fig. 2b). The indentations can also be seen in the images. The shape of the precipitates appears to be cubic in the joint center with an edge length in the range of 1 μm. In the base material the large particles are several microns in diameter and the fine precipitates are below 500 nm in size.

The atomic force microscope images of the joint and the base material of René N5 + NiGe20 are presented in Fig. 2c and d, respectively. It can be seen from Fig. 2c that the shape of the γ′-precipitates in the joint area is partially cubic with an approximate size of 1 μm. The size of the γ′-precipitates in the base material is below 1 μm and the shape of the particles is not cubic anymore. The microstructure here shows no sign of a pronounced bimodality.

3.2. Nanoindentation

The results of the nanoindentation experiments are shown in Fig. 3. In this diagram each data point represents at least 5 individual measurements in each phase. In Fig. 3a, the hardness of the γ and the γ′-phase in the initial gap region and the base material for PWA1483 + NiGe23 is plotted. The hardness in the matrix phase γ is almost identical in the gap region and the substrate material with a value of about 5.7–5.9 GPa. The hardness of the γ′-phase shows a bigger difference. Here the γ′-phase in the base material has a hardness of 9.7 GPa while in the gap a hardness of 8.6 GPa was found. This gives a γ′/γ hardness ratio of 1.5 in the gap center and of 1.6 in the base material. In the second generation superalloy René N5 the results are comparable to the previously presented PWA 1483 data. Also in this case the hardness of the matrix phase differs only slightly between gap region and base material. Here values of 6.8–6.9 GPa were measured within the gap and the base material. The difference for the γ′-phase is more pronounced with hardness values of 9.5 GPa in the parent material and 8.3 GPa in the joint region. The γ′/γ-hardness ratios are calculated to be 1.2 in the joint region and 1.4 in the base material.

The elastic modulus of the γ′ precipitate phase and the γ matrix in the base material and the joint region of PWA1483 + NiGe23 and Rene N5 + NiGe20 measured with the cube corner tip is in the range of 190–213 GPa. This is close to the modulus of PWA 1483 and René N5 measured by conventional nanoindentation at room temperature [4]. However due to the shape of cube corner tip, the elastic deformation is rather small compared to a Berkovich indenter and therefore an interpretation of the data is not reasonable.

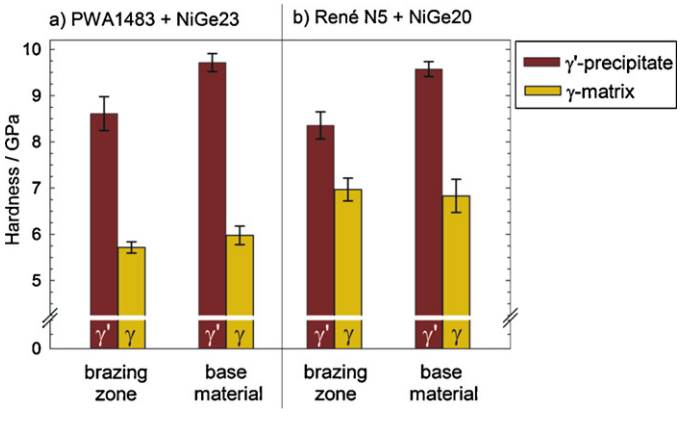

Fig. 3. Nanoindentation results for the brazings of (a)PWA 1483 + NiGe23 and (b)René N5 + NiGe20.

3.3. Lattice misfit

For both material systems a XRD scan was performed over the complete joint areas. From the diffraction angle the lattice parameters can be calculated according to Bragg's law. Although the beam width does not allow measurements with a lateral resolution high enough to measure the joint center separately, nevertheless significant differences of the lattice misfit between joint center and surrounding base material could be detected. In Fig. 4 the resulting plots of the intensity versus the lattice parameter over the joint region are shown for (a) PWA 1483 + NiGe23 and for (b) René N5 + NiGe20. It can be seen, that the width of the brazing affected zone is about 1 mm for both specimens. This corresponds well with the width of the diffusion affected zone of about 800 μm measured by electron probe micro analysis (EPMA) [4]. Also it is visible that within the former gap center the overall lattice parameter, i.e. the combined averaged parameter for γ and γ′, is lower than in the base material. In comparison with each other the mean value of the lattice parameter of the René N5 braze is slightly lower than for the PWA 1483 braze.

Fig. 5 shows selected diffraction profiles from measurements inside the joint center and in the base material for PWA 1483 and René N5, respectively. Within the figures the profiles, as recorded in the diffractometer, together with the de-convoluted sub-profiles for γ and γ′ are illustrated. For both regions in the PWA 1483 sample a negative lattice misfit is calculated, namely −0.09% for the joint center and −0.145% for the base material, respectively. Accordingly, in both regions the lattice parameter of the γ-matrix is higher than that of the γ′-phase, whereas both, γ and γ′, possess lower lattice parameters within the joint. In the joint center the mean lattice parameter is measured as 0.35835 nm compared to 0.3594 nm in the base material in PWA 1483.

For René N5 the mean lattice parameter does not vary strongly between joint and base material with 0.3580 nm and 0.35835 nm, respectively. Furthermore from the peak asymmetry of the combined profiles and the de-convoluted sub-profiles of γ and γ′ it is obvious that the misfit changes significantly. A negative misfit is found in the base material, whereas the misfit is positive in the joint region. It is clearly visible that this change can be ascribed to the strong change in the lattice parameter of the γ-phase. The resulting values for the misfit were +0.07% within the joint and −0.12% in the parent material.

3.4. EDX measurements

The overall chemical composition of the joint area and the base material was measured with the scanning electron microscope. The results are shown in Fig. 6. Due to the interdiffusion the compositions of the initially binary braze alloys is strongly altered. The concentration of alloying elements within the joint center of PWA 1483 + NiGe23 (Fig. 6a) and René N5 + NiGe20 (Fig. 6b) strongly increases compared to the pure braze alloy. The overall amount of alloying elements in the joint zone reaches up to half of that of the base material. Even for the rather slowly diffusing elements such as molybdenum and tungsten a significant presence within the joint area can be found, however less strongly concentrated. Especially rhenium is almost absent within the joint zone of René N5 + NiGe20 (Fig. 6b).

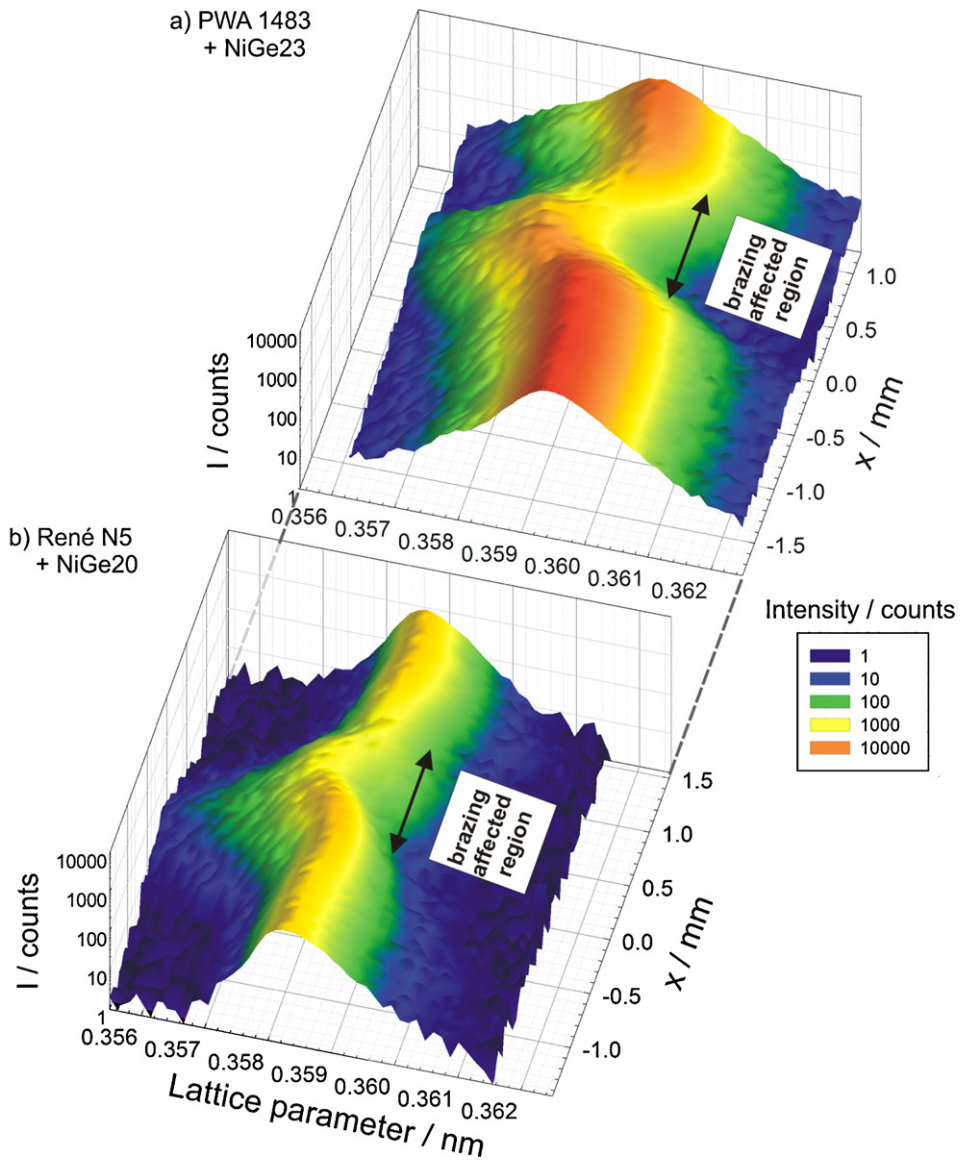

Fig. 4. Intensity plots of the (0 0 2) reflections over the brazing zones of (a) PWA 1483 + NiGe23 and (b) René N5 + NiGe20. The center of the brazing zone is at $x = 0$ mm.

The local concentration of the alloying elements in the γ matrix phase and the γ′ precipitate phase was determined by means of TEM-EDX. The concentration of Ge in the joint region of René N5 + NiGe20 is 6.6 at.% in the γ matrix phase and 8.5 at.% in the γ′ precipitate phase. Accordingly the partitioning coefficient for Ge $k^{\gamma'/\gamma}{}_{Ge}$, which is the ratio of the concentration of Ge in the γ′ precipitate phase to γ matrix phase, is of about 1.3. The partitioning coefficients of the other γ′ forming elements Ta and Al are 1.4 and 2.8, respectively, which means that Ge is more equally distributed than these both elements.

4. Discussion

The results from hardness and lattice misfit measurements are explained with respect to the changes of the local chemical compositions between base material and joint region, the partitioning behaviour of alloying elements and on the generally accepted knowledge concerning their influences on the properties of the phases γ and γ′.

4.1. Hardness

For the PWA 1483 + NiGe23 as well as for the René N5 + NiGe20 brazed samples a decreasing hardness of the γ′-phase from the base material to the joint region was found. This might be one reason why conventional nanoindentation experiments on the μm-scale show a reduced hardness in the joint area by about 10% [4].

The extent of this γ′-hardness reduction between base material and joint region is almost equal for both alloys. This decreasing hardness can be explained by a lower content of alloying elements in the γ′-phase in the joint region. Although pure Ni_3Ge is harder than Ni_3Al [14], it is known that the properties of Ni_3Al and also Ni_3Ge are very sensitive to alloying effects [15,16]. Alloying elements generally lead to an increase in flow stress in these materials [15]. Especially tantalum (Ta) is known to be a very potent strengthening element. Therefore the general decrease in hardness of the γ′-phase in the joint region compared to the base material is understandable due to the lower amount of elements which partitions to the γ′-precipitates, namely Ta and in the case of PWA 1483 also Ti. The fact that the hardness values for the γ′-phase in the base material of René N5 and PWA 1483 are almost identical although no Ti

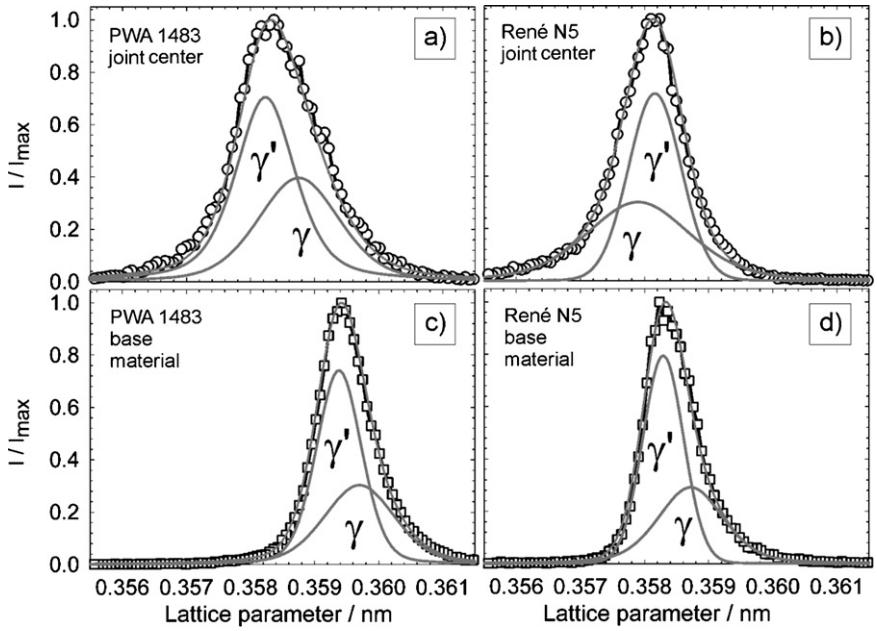

Fig. 5. XRD Profiles for the measurements within the joint region (a and b) and the base material (c and d) for PWA 1483 + NiGe23 (a and c) and René N5 + NiGe20 (b and d).

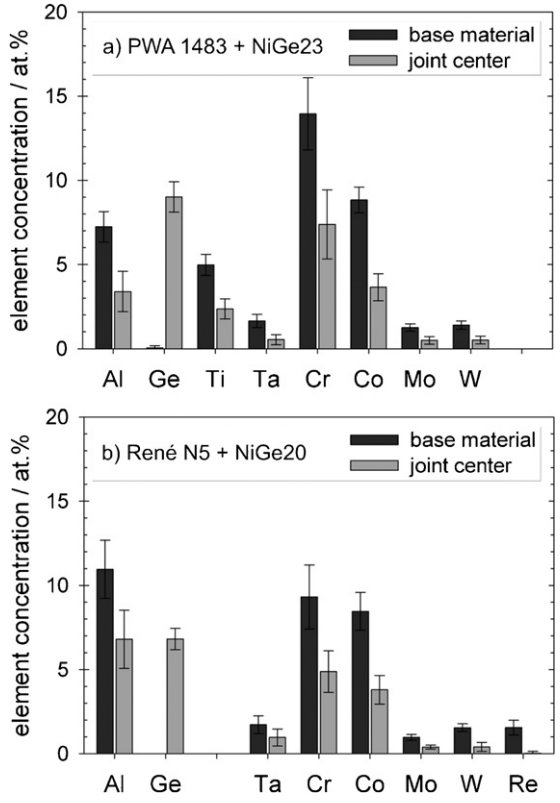

Fig. 6. Results of the EDX analysis of the two brazing of (a) PWA 1483 + NiGe23 and (b) René N5 + NiGe20. Plotted are base material and the joint center for both systems.

is alloyed in Rene N5 can be explained by the higher content of Ta in the alloy René N5.

When comparing the hardness of the γ-matrix phase in the joint region with the hardness of the γ-matrix phase in the base material no distinct trend can be observed here in both alloys. The nanoindentation measurements in the joint area as well as in the base material yield comparable results, even though the amount of solid solution strengthening alloying elements within the joint region is strongly reduced compared to the base material. The conceivable reasons for this are manifold. As can be seen from the AFM images, the shape of the precipitates within the joint region is more cubic, whereas in the base material it has already changed to a more irregular morphology.

This can be explained by the high process temperatures and the thermophysical properties of the alloys. The γ′ solvus temperature of PWA 1483, as calculated by ThermoCalc (database TTNi7), is 1170 °C and only 10 °C higher than the brazing temperature of 1160 °C for PWA 1483 + NiGe23. Accordingly the γ′ precipitates dissolve and only a very small γ′-volume fraction is present. During the brazing process the remaining γ′-precipitates coarsen strongly. The subsequent cooling leads to the precipitation of smaller γ′-precipitates in the γ-matrix and a bimodal microstructure in the base material. In contrary the calculated γ′ solvus temperature of Rene N5 is 1270 °C and 70 °C higher than the brazing temperature of 1200 °C for Rene N5 + NiGe20. As a consequence of the higher γ′-volume fraction at the brazing process the microstructure is more uniform. However in both base materials the γ′-precipitates possess a largely irregular morphology.

This irregular morphology in connection with the lattice mismatch measurements leads to the assumption that the γ′-precipitates in the base material are already incoherent or semicoherent relative to the matrix. This could be expected as they were exposed to a high temperature for an extended time period during the brazing process. It is known that this will lead to coarsening and the development of interfacial dislocations at the precipitate/matrix interfaces [17]. Whereas the γ′-precipitates in the joint are either coherently embedded in the matrix or at least the loss of coherency is not as pronounced since the γ′-precipitates had been formed during the brazing process and the interfacial dislocation network were not developed fully yet. Consequently, the coherency stresses within the γ/γ′ interfaces are more pronounced in the joint center. This could lead to an additional hardening effect.

Other possible reasons are the presence of secondary γ′ precipitates and the γ/γ′ partitioning behaviour of Ge in the joint region. The TEM-EDX measurements on Rene N5 + NiGe20 show that Ge partitions more equally between γ and γ′ than Al and Ta. This leads to a high concentration of Ge in the γ phase which acts as a solid solution hardening element in the γ matrix.

In the base material of René N5 + NiGe20 the hardness of the γ-phase is distinctively higher than in the base material of PWA 1483 + NiGe23. This can be rationalized by the presence of rhenium in Rene N5. As rhenium is known to be a very potent solid solution strengthening element for nickel [7,8] it probably also compensates for the lower chromium content of Rene N5. Therefore this increase in hardness for the matrix phase in the base material compared to PWA 1483 is easily understood. However, only a very small amount of rhenium is present in the joint center. It is unknown, if one of the above mentioned possibilities, like the high concentration of Ge in the γ matrix is responsible for the high hardness of the γ matrix in the joint region of the Rene N5 brazed sample. The hardness ratios determined in the base material of PWA 1483 + NiGe23 and René N5 + NiGe20, respectively are also in good agreement with values reported for other first and second generation superalloys in literature, e.g. CMSX-6 and CMSX-4 [7].

4.2. Lattice parameter and misfit

The first generation superalloy PWA 1483 exhibits significantly higher lattice parameters of both the γ-matrix as well as the γ′-phase compared to the second generation superalloy René N5. This can be explained by the addition of Ti and the considerably higher amounts of Cr in PWA 1483. Ti and Cr are known to partition predominantly to γ′- in the case of Ti and to the γ-phase in the case of Cr [8,18]. It is also reported in literature that both elements increase the lattice parameter of the respective phase [19]. In the base material of both alloys the lattice misfit is negative with values of −0.145% (PWA 1483) and −0.12% (René N5). However significant differences in the lattice misfit of the joint region can be found in both alloys. Interestingly, while the lattice mismatch in the joint area of PWA 1483 + NiGe23 is negative as in the base material it is positive in the joint region of the Rene N5 + NiGe20. Fig. 4 shows that within the joint area of both alloys the lattice parameters of both γ and γ′ are decreased which result from the lower overall content of alloying elements such as Ti, Ta, Cr, Mo, W and Re compared to the base material (see Fig. 6). In general, the lattice parameter for the pure element and binary precipitate phases Ni, Ni_3Al and Ni_3Ge, which has a value of about 0.3516 nm [18], 0.3571 nm [20] and 0.3567 nm [21], is lower than the values for the γ- matrix and γ′-precipitates in typical alloys.

Since the lattice parameter of the γ′-phase in the joint area is almost similar in both alloys, the pronounced change of the lattice misfit compared with the base material is caused by differences in the lattice parameter of the γ-phase, as visible in Fig. 5. This is a consequence especially of the alloying elements Cr and Re. PWA 1483 has a much higher content of Cr than René N5 and Cr has a much higher diffusivity in Ni than Re [22]. Consequently after the brazing heat treatment a significant amount of Cr has diffused from the base material to the joint area in the PWA 1483 + NiGe23 and the lattice parameter of the γ-phase in the joint region and base material is nearly equal. On the contrary in the case of the René N5 + NiGe20 just a negligible amount of Re has diffused to the joint area and the lattice parameter of the γ-phase is lower than in the base material and also lower than the lattice parameter of γ′-phase.

The switch from the negative misfit in the base material to the positive misfit in the joint area in René 5 + NiGe20 has also consequences for the evolution of the γ/γ′-microstructure during creep deformation. First creep tests under compression at 1000 °C with applied loads of 200 MPa for René N5 + NiGe20 and 150 MPa for PWA 1483 + NiGe23 resulted in a directional coarsening of the γ′-precipitates perpendicular to the external applied load in the joint region of Rene N5 + NiGe20 and parallel in the joint region of PWA 1483 + NiGe23, respectively (Fig. 7). For both alloys parallel coarsening of the γ′-precipitates was observed in the base material. If γ′-particles coarsen parallel or perpendicular to the external load depends on the character of the creep load, being either compressive or tensile, and the sign of the lattice misfit [10]. Under compressive load as applied in these tests parallel coarsening is found for negative lattice misfit. This corresponds with the misfit measured in the base materials of PWA 1483 and Rene N5 as well as in the joint region of PWA 1483 + NiGe23. Perpendicular coarsening of the γ′-particles corresponds with the positive lattice misfit measured in the joint area of Rene N5 + NiGe20. In summary, this different microstructural evolution in the joint regions during creep confirms clearly the opposite sign of the local lattice misfit of René N5 + NiGe20 (positive) and PWA 1483 + NiGe23 (negative) measured by XRD. The result that the diffusion process leads to different directional rafting is of great importance as, in addition to the solid solution hardening, the direction of the rafted microstructure might influence the mechanical properties of the joint region as well. A more detailed description of these creep tests will be published elsewhere.

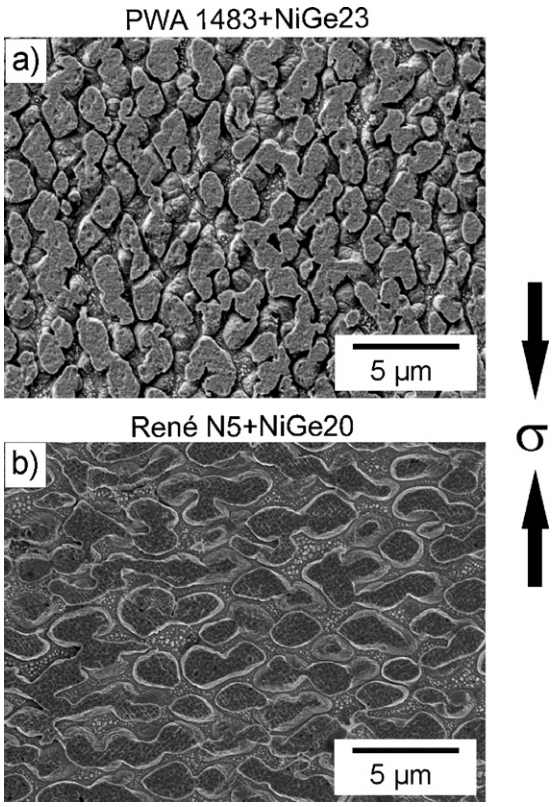

Fig. 7. Microstructure in the joint region after creep under compression at 1000 °C with applied loads of (a) 150 MPa for PWA 1483 + NiGe23 and (b) 200 MPa for René N5 + NiGe20.

5. Conclusions

The investigation on the local properties of single crystalline brazing joints in two nickel-base superalloys revealed the following:

- The microstructure within the joint consists of a γ matrix and $L1_2$-precipitates.
- The measurements with the NI-AFM show reduced hardness for the γ′-precipitates in the joint area relative to the base material for both alloy systems.
- The hardness of the γ-matrix is comparable in the joint area and the base material for both alloy systems.

– In PWA 1483 + NiGe23 the lattice misfit is negative both in the joint as well as in the base material. This leads to a directional coarsening parallel to the external applied compressive load in the joint region of PWA 1483. The absolute lattice parameters of both phases γ and γ' are reduced in the joint area compared to the base material.
– In René N5 + NiGe20 the lattice misfit is negative in the base material, but is found to be positive in the joint area. This is mainly caused by the relatively low lattice parameter of the γ-matrix due to negligible diffusion of rhenium from the base material to the joint area. This leads to a directional coarsening perpendicular to the external applied compressive load in the joint region of Rene N5.

Acknowledgments

Financial grants from the German Research Foundation (DFG) in the frame of the research training group 1229, the Bavarian Research Foundation and the Bavarian State Ministry of Sciences, Research and the Arts are gratefully acknowledged. The authors thank Siemens AG Power Generation (M. Ott), MTU Aero Engines GmbH (E. Affeldt) and MTU Maintenance Hannover GmbH (A. Vossberg) for supplying the investigated alloys and the Institute of Science and Technology of Metals of Professor Singer at the University Erlangen-Nürnberg for brazing the alloys. The authors also thank the group of Dr. Cathie Rae and Dr. Howard Stone at the Rolls-Royce University Technology Centre and Mary Vickers at the X-ray Facility at the University of Cambridge where one of the authors (S. Neumeier) performed the XRD measurements.

References

[1] D. Kim, K. Nishimoto, Met. Mater. Int. 8 (2002) 403–410.
[2] A. Schnell, PhD Thesis, Ecole Polytechnique Fédérale de Lausanne, 2004.
[3] S.K. Tung, L.C. Lim, M.O. Lai, Scripta Mater. 34 (1996) 763–769.
[4] M. Dinkel, P. Heinz, F. Pyczak, A. Volek, M. Ott, E. Affeldt, A. Vossberg, M. Göken, R.F. Singer, in: R.C. Reed (Ed.), Proceedings of the 11th International Symposium, TMS, Warrendale, PA, 2008, pp. 211–220.
[5] P. Heinz, PhD Thesis, University Erlangen-Nürnberg, 2009.
[6] M. Göken, M. Kempf, Acta Mater. 47 (1999) 1043.
[7] K. Durst, M. Göken, Mater. Sci. Eng. A 387–389 (2004) 312–316.
[8] S. Neumeier, F. Pyczak, M. Göken, in: R.C. Reed (Ed.), Proceedings of the 11th International Symposium, TMS, Warrendale, PA, 2008, pp. 109–119.
[9] R.A. MacKay, L.J. Ebert, Scripta Metall. 17 (1983) 1217.
[10] H. Mughrabi, Mater. Sci. Tech. 25 (2009) 191–204.
[11] W.C. Oliver, G.M. Pharr, J. Mater. Res. 7 (1992) 1564–1583.
[12] T. Schöberl, H.S. Gupta, P. Fratzl, Mater. Sci. Eng. A 363 (2003) 211–220.
[13] A. Royer, P. Bastie, M. Veron, Acta Mater. 46 (1998) 5357.
[14] D.M. Wee, T. Suzuki, Trans. Jpn. Inst. Metals 20 (1979) 634–646.
[15] D.H. Pope, S.S. Ezz, Int. Metals Rev. 29 (1984) 136.
[16] N.S. Stoloff, Int. Mater. Rev. 34 (1989) 153.
[17] M. Feller-Kniepmeier, T. Link, Mater. Sci. Eng. A 113 (1989) 191–195.
[18] F. Pyczak, B. Devrient, H. Mughrabi, in: K.A. Green (Ed.), Proceedings of the 10th International Symposium, TMS, Warrendale, PA, 2004, pp. 827–836.
[19] P. Caron, in: T.M. Pollock (Ed.), Proceedings of the 9th International Symposium, TMS, Warrendale, PA, 2000, pp. 737–746.
[20] W.B. Pearson, Handbook of Lattice Spacings and Structures of Metals and Alloys, Vol. 1+2, Pergamon Press, Oxford, 1967.
[21] P.V.M. Rao, S.V. Suryanarayana, K.S. Murthy, S.V.N. Naidu, J. Phys. Condens. Matter. l (1989) 5357–5361.
[22] M.S.A. Karunaratne, et al., in: T.M. Pollock (Ed.), Proceedings of the 9th International Symposium, TMS, Warrendale, PA, 2000, pp. 263–272.